catalysts

MDPI

Article

The Effect of Potassium on Cobalt-Based Fischer–Tropsch Catalysts with Different Cobalt Particle Sizes

Ljubiša Gavrilović, Jonas Save and Edd A. Blekkan *

Department of Chemical Engineering, Norwegian University of Science and Technology, Sem Sælands vei 4, 7491 Trondheim, Norway; ljubisa.gavrilovic@ntnu.no (L.G.); jonassave@gmail.com (J.S.)

* Correspondence: edd.a.blekkan@ntnu.no; Tel.: +47-7359-4157

Received: 15 February 2019; Accepted: 8 April 2019; Published: 10 April 2019

Abstract: The effect of K on 20%Co/0.5%Re/γ-Al_2O_3 Fischer–Tropsch catalysts with two different cobalt particle sizes (small, in the range 6–7 nm and medium size, in the range 12–13 nm) was investigated. The catalyst with the smaller cobalt particle size had a lower catalytic activity and C_{5+} selectivity while selectivities towards CH_4 and CO_2 were slightly higher than over the catalyst with larger particles. These effects are ascribed to lower hydrogen concentration on the surface as well as the lower reducibility of smaller cobalt particles. Upon potassium addition all samples showed decreased catalytic activity, reported as Site Time Yield (STY), increased C_{5+} and CO_2 selectivities, and a decrease in CH_4 selectivity. There was no difference in the effect of potassium between the sample with small cobalt particles compared to the sample with medium size particles). In both cases the specific activity (STY) fell and the C_{5+} selectivity increased in a similar fashion.

Keywords: Fischer–Tropsch; cobalt; catalyst deactivation; potassium

1. Introduction

Biomass to liquid (BTL) via gasification and integrated Fischer–Tropsch synthesis (FTS) is an attractive process for the production of green diesel and jet fuel [1]. The first step involves biomass gasification to produce syngas (CO + H_2) [2]. It was reported [3] that impurities in biomass feedstocks and partial gasification can lead to contaminants (such as: tars, alkali, HCN, H_2S, etc.) in the produced syngas, which might cause catalyst deactivation and other problems downstream. Therefore, a series of cleaning steps must be applied to fulfil the requirement for pure gas before entering the FTS reactor [4]. Alkali salts (mainly potassium) are the dominant salts in fly ash composition after biomass gasification [5]. Due to poor plant design or imperfections in the cleaning section, these alkali salts might be present in the gas when entering the FTS section [6]. It was previously reported that alkali has a strong negative effect on FTS activity on Co-based catalyst [7–12]. Poisoned samples were characterized carefully, but none of the standard techniques applied showed significant differences between the reference (unpoisoned) and poisoned samples. Hence, the catalyst loss in activity and changes in selectivity that was observed were explained by the hypothesis that potassium is able to move to the cobalt sites responsible for FTS when reactions or the pre-treatment conditions are reached [11–13]. The mobility of potassium species under reaction conditions has been demonstrated in other systems [14], where the transport mechanism was suggested to involve OH-groups on the surface. Once the potassium reaches the cobalt particles there are very low barriers against transport on the cobalt surface, as calculated using DFT, and the adsorption of K is favourable on all sites, including sites such as the B_5 and B_6 sites often considered active sites for the FTS [15].

The effect of Co particle size on cobalt-based FT catalysts have been studied extensively [16–19]. A decreased turnover frequency (TOF) and increased methane selectivity has been found for FTS

experiments (performed at 1 and 35 bar (H_2/CO = 2)) for catalysts with Co particles smaller than around 6 nm [18]. With decreasing Co particle size the fraction of sites that are less coordinated (like steps, kinks, edges, and corners [20]) increases.

To better understand the nature of the effects reported on the cobalt-based FTS catalysts upon alkali addition, here we report an investigation of the effect of potassium on alumina-supported cobalt catalysts containing small or medium sized cobalt particles. A difference in the behavior could give information on the nature of K poisoning, and on the role of various sites on the cobalt surface.

2. Results

Two alumina-supported catalysts, with different cobalt particle sizes, were prepared using the incipient wetness impregnation technique. During the impregnation process, the pores of the support are filled with the active metal solution by means of capillary forces. Thus, the particle size of the active metal is determined during the drying procedure [21]. To be able to alter the particle size of the active metal, one needs to use support with the wider pores, like α-Al_2O_3, since the wider pores will consequently give a bigger particle size. By mixing the solvent (water) with ethylene glycol (EG) during the impregnation step, a smaller cobalt particle size was achieved. In this way, the cobalt particle size was successfully altered without changing the composition of the active material or the physical properties of the support material. A summary of the characterization results is presented in Table 1. Both the X-ray diffraction (XRD) and H_2-chemisorption experiments showed decreased particle size for the catalyst prepared using EG (Cat2). This catalyst (Cat2) showed higher dispersion (15.6 %) and consequently reduced particle size compared to the Cat1 (D = 7.7 %) (prepared without EG) measured by H_2-chemisorption. XRD measurements confirmed the reduction in Co_3O_4 particle size from ~15 nm to ~5 nm upon ethylene glycol addition. The XRD profiles of all the catalyst with different potassium loadings are illustrated in Figures 1 and 2. All the samples showed existence of the cubic Co_3O_4 and Al_2O_3 phases, while potassium is not visible due to the low concentration. No difference can be detected in the size or shape of the peaks regardless of potassium concentration, Figure 1. Upon EG addition, all the Co_3O_4 peaks are broadened and less pronounced, while the Al_2O_3 peaks become sharpened and more pronounced, Figure 2. This is in agreement with previously published work where cobalt particle size was also altered using EG [16,17]. It was explained by EG acting mainly as a surfactant, thus increasing the wetting ability of the cobalt salt solutions. Borg et al. [17] showed, using transmission electron microscopy (TEM) images, that Co_3O_4 crystallites appeared in aggregates with dimensions above 100 nm with pure water as a solvent, while the aggregates were absent when EG was used.

Table 1. Characterization results.

Catalyst	K Impurity (ppm)	D [a] (%)	d(Co^0) [b] (nm)	BET Surface Area [c] (m^2/g)	Average Pore Diameter (nm)	Pore Volume (cm^3/g)	d(Co_3O_4) [d] (nm)	d(Co^0) [d] (nm)
Cat1	6	7.7	12.5	145	13.7	0.60	14.8	11.1
Cat1	551	7.7	12.5	137	12.2	0.46	15	11.3
Cat1	902	7.3	13.3	137	12.4	0.47	17.2	12.9
Cat2	15	15.6	6.2	143	12.2	0.52	4.9	3.7
Cat2	471	14.3	6.7	143	12.4	0.53	4.6	3.5
Cat2	886	15.1	6.4	152	10.6	0.48	4.8	3.6

[a] Standard deviation 3.3%; [b] Found by H_2-chemisorption; [c] Standard deviation 4.7%; [d] Found by X-ray diffraction (XRD) experiments.

Upon alkali addition, no significant differences are observed between Cat1 and Cat2. The measured potassium loadings are close to the nominal values. The low level measured for the samples without added potassium is due to the support containing traces of K. The particle size estimates did not change upon the addition of potassium. All the catalysts showed almost the same surface area (~140 m^2/g), pore size (~0.5 nm), pore volume (~12 cm^3/g), regardless of the EG or K loading, the deviations

being within experimental error. These catalyst morphological findings are similar to our previously published work with alkali poisoning [11].

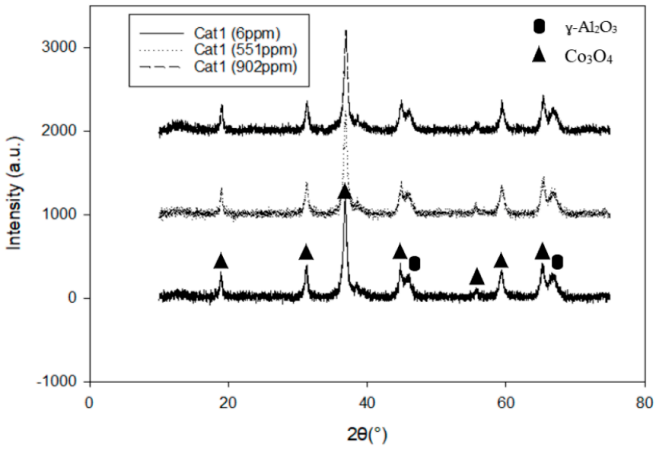

Figure 1. XRD patterns for 20%Co/0.5%Re/γ-Al_2O_3 with different K loadings.

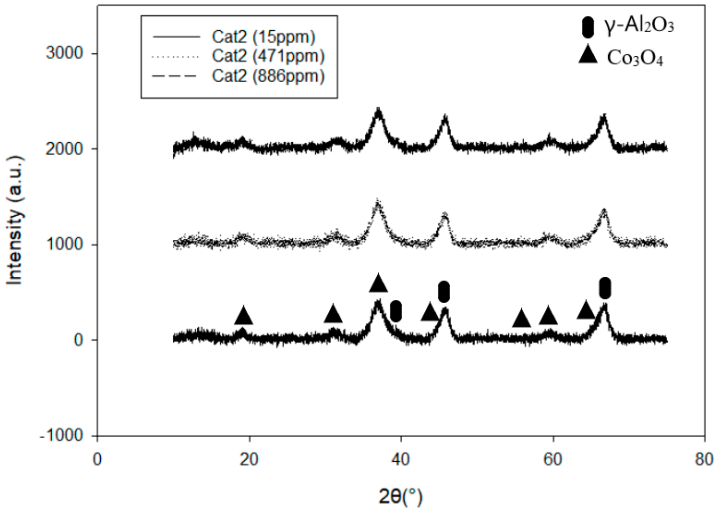

Figure 2. XRD patterns for 20%Co/0.5%Re/γ-Al_2O_3 with different K loadings.

Temperature-programmed reduction (TPR) profiles of the catalysts Cat1 and Cat2 with different K loadings are presented in Figure 3. All the samples showed a typical reduction profile often observed for alumina supported Co catalyst [22]. The small first peak (around 220 °C) visible for some of the catalysts represents the reduction and removal of residual nitrates from the cobalt precursor [23]. Two main peaks at ~330 °C and ~430 °C are referred to the transition from Co_3O_4 to CoO and CoO to metallic Co, respectively [22]. The peak temperature of the first reduction peak was slightly decreased to ~290 °C, while the second reduction peak was shifted to slightly higher temperatures (~490 °C) for the catalyst prepared with EG. This is related to the particle size effect, indicating a more difficult reduction to metallic cobalt, which was earlier reported by Jacobs et al. [24]. A lower degree of reduction has also been reported for cobalt-based FT catalysts of similar particle sizes [17,25]. A slight shoulder can be seen on the second reduction peak for the catalyst prepared with EG. Borg et al. [26] ascribed this phenomenon to a larger spread in the particle size distribution, indicating a large variation in the degree of interaction between particles and the support. There is no difference upon K addition, all the samples follow the same trend as the unpoisoned catalysts, which is a similar observation as in previously published work focusing on medium-sized cobalt particles only [9,12].

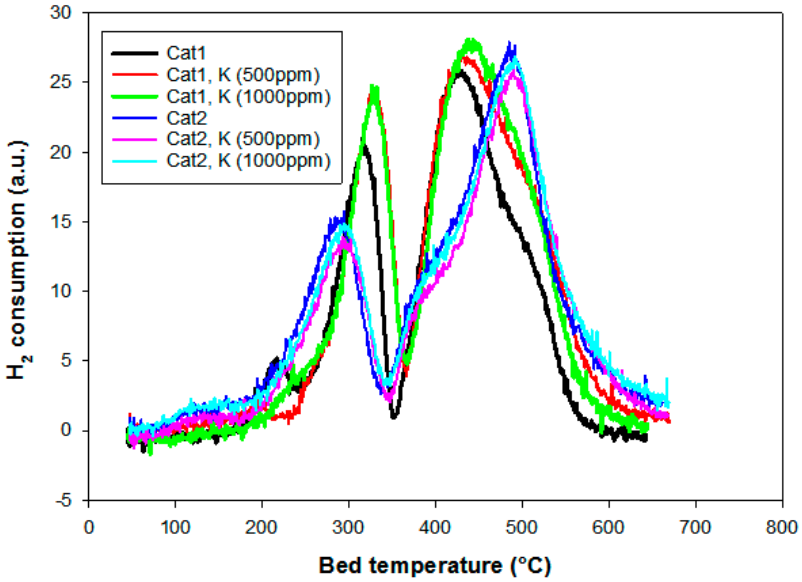

Figure 3. Temperature-programmed reduction (TPR) profiles of the catalysts Cat1 and Cat2 with different K loadings.

The Fischer–Tropsch activity and selectivity results are presented in Table 2. Catalyst activity measured as STY was found to be 0.054 to 0.027 s^{-1} for the Cat1 and Cat2 catalysts with Co particle sizes of ~13 and ~6 nm respectively. The smaller cobalt particles also give significantly lower C_{5+} selectivity and higher CH_4 and CO_2. It is previously reported that catalyst activity on supported cobalt catalysts is considered independent of cobalt dispersion [27] and support identity [28], but this only holds for larger cobalt particles. Bezemer et al. [18] reported a strong influence of the cobalt particle size (in the range 3 to 8 nm) on both the cobalt site-time yield and the C_{5+} selectivity using carbon nanofibers as a support. The cobalt particle size effect was explained as a combination of CO-induced surface reconstruction and non-classical structure sensitivity. In the present work, γ-alumina is used as the catalyst support, and we observe the same particle size effect on the catalyst activity and selectivity, in agreement with Borg et al. [17]. Wang et al. [29] showed that for very small Co particles (1.4–2.5 nm), the Co surface was readily oxidized by water vapor, while for the larger Co particles (3.5–10.5 nm), such oxidation was not evident. This was confirmed by Azzam et al. [30] where the poor catalyst activity and higher CH_4 and CO_2 selectivities for the very small particles (1 nm) was ascribed to catalyst oxidation by water. However, in the present work the particle size is in the range 6–13 nm indicating that oxidation is not the reason for the dramatic effect in the specific activity. Yang et al. [16] also reported increased turnover frequency (TOF) with increasing cobalt particle size. They explained the effect by the increased CO coverage which is directly proportional with increasing Co particle size. Den Brejeen et al. [31] reported, using SSITKA experiments, that small cobalt particles have higher coverage of 'irreversible' adsorbed CO, which can block the surface and lead to lower activity, while the coverage of H is increased which leads to more methane production.

The activity decreases severely upon increased K loading for both catalysts. The loss in specific activity with the potassium loading is similar for the two samples, losing approximately 30% of the activity with the highest K loading. The changes in catalytic activity are similar to those observed previously [9–13].

Also in terms of selectivity is there little difference in the response to the potassium loading between the two samples. Both catalysts showed increased C_{5+} and CO_2, and decreased CH_4 selectivity upon K addition. Hence, the effect of potassium is the same independent of the cobalt particle size in the range investigated here.

The main conclusion from this work is that K effects the cobalt based catalyst in the same way for two distinctly different cobalt particle sizes. Although the catalyst with smaller particle size (Cat2)

showed lower activity and a poorer selectivity, the K effect appears to be independent of Co particle size. We have previously shown that step sites are preferred sites for CO and K adsorption [15], but the difference between facets is small and the adsorption of K is energetically favored on all sites on the cobalt surface. The smaller particles investigated here are likely to have a slightly larger fraction of step and edge sites, but the difference is perhaps not large enough to be significant.

Table 2. Catalytic activity reported as site time yield (STY) and selectivities to C_{5+}, CH_4 and CO_2 with different catalyst and potassium loadings (Calculation procedures see the Supplementary Materials).

Catalyst	K (ppm)	STY (s^{-1}) [a]	C_{5+} (%)	CH_4 (%)	CO_2 (%)
Cat1	6	0.054	85.4	7.3	0.16
Cat1	551	0.041	86.6	6.8	0.23
Cat1	902	0.039	86.3	6.7	0.40
Cat2	15	0.027	79.3	10	0.23
Cat2	471	0.022	83.1	9.5	0.39
Cat2	886	0.019	81.0	9.2	0.55

[a] Standard deviation ± 7%.

3. Materials and Methods

The 20%Co/0.5%Re/γ-Al_2O_3 catalyst was prepared using a one-step incipient wetness impregnation of an aqueous solution of $Co(NO_3)\cdot 6H_2O$ and $HReO_4$ [10]. The catalyst support was from Sasol (Puralox γ-alumina). The catalyst was then dried in a stationary oven at 120 °C for 1 h. The calcination procedure in flowing air in a fixed bed quartz reactor at 300 °C for 16 h, using a ramp rate of 2 °C/min was applied after drying. Finally, the oxidized catalyst precursors were sieved to a particle range of 53–90 μs. The prepared catalyst should be free from impurities, but by analysis a small amount of K was found in the support (6 and 15 ppm) [26]. In order to achieve different particle sizes, a method using mixtures of distilled water and ethylene glycol (EG) in the impregnation solution was used [17]. One sample was prepared using only water as the solvent (Cat1), the second sample was prepared using a mixture of 80 wt% water and 20 wt% EG (Cat2), the latter sample is expected to have a smaller cobalt particle size. These two samples (in their calcined state) were post-impregnated with 500 and 1000 ppm of potassium in the form of KNO_3 dissolved in deionized water. Inductively coupled plasma–mass spectrometry (ICP–MS) was used to analyze the amount of potassium present in the catalysts. The catalysts samples were dried and calcined using the same conditions both after the initial preparation and after post-impregnation with potassium.

In order to determine surface area, pore volume and average pore diameter of the prepared catalysts, a Tristar II 3020 was used to perform a volumetric adsorption of N_2. Prior to the measurement at liquid nitrogen temperature, the catalyst samples (~70 mg, 53-90 μm) were outgassed in vacuum, first at room temperature for 1h and then at 200 °C overnight. For calculation of the surface area the Brunauer–Emmet–Teller (BET) [32] isotherm was used while to determine a pore volumes and average pore diameters of the samples the Barret–Joyner–Halenda (BJH) [33] method was applied.

H_2-chemisorption was carried out using a Micromeritics ASAP2010 unit. The catalyst sample (0.2 g) was placed between quartz wool wads and loaded in the chemisorption reactor. Before the measurements, the sample was reduced in flowing hydrogen at 350 °C for 16h with a ramping rate of 60 °C/h After reduction, the analysed samples were cooled to 30 °C under vacuum. Chemisorption data was obtained at 30 °C between 0.020 and 0.667 bar H_2 pressure. It was presumed that for each surface cobalt atom there was one H chemisorption site and that neither Re, K nor the support contributed to chemisorption. The particle sizes (in nm) were estimated using the following equation [34], where *D* is cobalt dispersion in %:

$$d\left(Co^0\right) = \frac{96.2}{D}$$

TPR experiments were carried out in the Altamira AMI-300RHP. The catalyst sample (100 mg) was loaded between wads of quartz wool and placed in a quartz u-tube reactor. Prior the measurement,

the catalyst was treated in inert gas at 200 °C. The catalyst was then reduced in hydrogen flow (7% H_2/Ar 50 ml/min) to a temperature of 700 °C with a ramp rate of 10 °C/min. Finally, the samples were cooled down to ambient temperature.

A D8 DaVinci-1 X-ray Diffractometer with CuKα radiation was used for all XRD experiments. The analysis was run for 60 min for each catalyst sample, examining a range of 2θ from 10 to 75° at a step size of 0.013° while using the X-ray source at 40 kV and 40 mA. The average cobalt oxide crystallite thickness was calculated by Scherrer's equation [35] using the (311) Co_3O_4 peak located at 2θ = 36.8°, and applying a K-factor of 0.89. Subsequently, the metallic cobalt particle size was estimated using the relative volume contraction between Co_3O_4 and metallic cobalt [36]:

$$d\left(Co^0\right) = 0.75d(Co_3O_4)$$

Fischer–Tropsch experiments wer perfomed in 10 mm ID steel tube fixed bed reactor at industrially relevant conditions (210 °C, 20 bar and a H_2/CO ratio of 2.1). The catalyst samples (1 g) were mixed with inert SiC (20 g) and loaded between quartz wool wads to fix the location in the reactor. To improve the heat distribution, aluminium blocks were placed around the reactor. The reactor was then placed in an electrically heated furnace. Before hydrogen reduction, a leak test with He was performed. The *in situ* reduction was carried out at 350 °C for 10 h with a ramp rate of 1 °C/min from ambient temperature. After reduction, the samples were cooled to 170 °C. Prior to the syngas introduction (250 Nml/min), He was used to build up a pressure to 20 bar. The temperature program was set to increase the temperature first from 170 to 190 °C and then to the final temperature of 210 °C with ramping rates of 20 °C/min and 5 °C/min, respectively. Liquid Fischer–Tropsch products were separated in a hot trap at ~87 °C and a cold trap at ambient temperature. Wax was collected in the hot trap while other liquids (water and light hydrocarbons) were collected in the cold pot at. The C_1-C_4 gases were analyzed using a HP 6890 gas chromatograph. N_2 (internal standard), H_2, CO, CH_4 and CO_2 were analyzed on a TCD following separation on a Carbosieve column. Hydrocarbon products were separated with a GS-Alumina PLOT column and detected on a flame ionization detector (FID). CH_4 was used to combine TCD and FID analysis in the calculations. The syngas contained 3 % N_2 which is used as an internal standard for quantification of the products to close the mass balance. Activity data were reported based on measurements at constant feed rate (250 Nml/min) after 24 h time on stream. Then the syngas flow was changed to obtain ~50 % CO conversion. Selectivity data are reported at 50 ± 5% CO conversion based on the analysis of C_1–C_4 hydrocarbons in gas phase after ~48 h time-on-stream. Since the focus is on the amount of higher hydrocarbons, the selectivity is reported in the usual way as C_{5+} and CH_4 selectivity.

4. Conclusions

The effect of potassium on Co-based FT catalysts was examined on two different particle sizes of cobalt, small and medium. The catalyst activity decreased with decreased particle size, while the morphological characteristics are unchanged. The C_{5+} selectivity decreased, while CH_4 and CO_2 increased for the catalyst with smaller particle size. Upon potassium addition there was no change in dispersion, surface area, pore size, pore volume, regardless of the particle size or potassium concentration. However, all the catalysts showed a negative effect of K on catalyst activity. C_{5+} selectivity was increased, while methane and CO_2 decreased with increasing K concentration. There was no difference in the potassium effect regarding the particle size, indicating that the catalytic performance was affected in the same fashion.

Supplementary Materials: The following are available online at http://www.mdpi.com/2073-4344/9/4/351/s1, Calculation procedures, 1.1. Site time yield; 1.2. Selectivities.

Author Contributions: Conceptualization, E.A.B. and L.G.; methodology, J.S. and L.G.; investigation, J.S.; data curation, J.S.; original draft preparation, L.G.; writing—review and editing E.A.B.; supervision, E.A.B.; project administration, E.A.B.; funding acquisition, E.A.B.

Funding: We thank the Research Council of Norway for funding (contracts no: 228741, 257622, 280846).

Conflicts of Interest: The authors declare no conflict of interest.

References

1. Rauch, R.; Kiennemann, A.; Sauciuc, A. Fischer-Tropsch Synthesis to Biofuels (BtL Process). In *The Role of Catalysis for the Sustainable Production of Bio-Fuels and Bio-Chemicals*; Elsevier Inc.: Amsterdam, The Netherlands, 2013; pp. 397–443.
2. van Steen, E.; Claeys, M. Fischer-Tropsch catalysts for the biomass-to-liquid process. *Chem. Eng. Technol.* **2008**, *31*, 655–666. [CrossRef]
3. Woolcock, P.J.; Brown, R.C. A review of cleaning technologies for biomass-derived syngas. *Biomass Bioenergy* **2013**, *52*, 54–84. [CrossRef]
4. Boerrigter, H.; Calis, H.P.; Slor, D.J.; Bodenstaff, H. Gas Cleaning for Integrated Biomass Gasification (Bg) and Fischer-Tropsch (Ft) Systems; Experimental Demonstration of Two Bg-Ft Systems. In Proceedings of the 2nd World Conference and Technology Exhibition on Biomass for Energy, Industry and Climate Protection, Rome, Italy, 10–14 May 2004.
5. Norheim, A.; Lindberg, D.; Hustad, J.E.; Backman, R. Equilibrium calculations of the composition of trace compounds from biomass gasification in the solid oxide fuel cell operating temperature interval. *Energy Fuels* **2009**, *23*, 920–925. [CrossRef]
6. Boerrigter, H.; Calis, H.-P.; Uil, H.D. Green Diesel from Biomass via Fischer-Tropsch synthesis: New Insights in Gas Cleaning and Process Design. In Proceedings of the Pyrolysis and Gasification of Biomass and Waste, Strasbourg, France, 30 September–1 October 2002; pp. 1–13.
7. Tristantini, D.; Lögdberg, S.; Gevert, B.; Borg, Ø.; Holmen, A. The effect of synthesis gas composition on the Fischer-Tropsch synthesis over Co/γ-Al_2O_3 and Co-Re/γ-Al_2O_3 catalysts. *Fuel Process. Technol.* **2007**, *88*, 643–649. [CrossRef]
8. Borg, Ø.; Hammer, N.; Enger, B.C.; Myrstad, R.; Lindvåg, O.A.; Eri, S.; Skagseth, T.H.; Rytter, E. Effect of biomass-derived synthesis gas impurity elements on cobalt Fischer-Tropsch catalyst performance including in situ sulphur and nitrogen addition. *J. Catal.* **2011**, *279*, 163–173. [CrossRef]
9. Balonek, C.M.; Lillebø, A.H.; Rane, S.; Rytter, E.; Schmidt, L.D.; Holmen, A. Effect of alkali metal impurities on Co-Re catalysts for Fischer-Tropsch synthesis from biomass-derived syngas. *Catal. Lett.* **2010**, *138*, 8–13. [CrossRef]
10. Lillebø, A.H.; Patanou, E.; Yang, J.; Blekkan, E.A.; Holmen, A. The effect of alkali and alkaline earth elements on cobalt based Fischer-Tropsch catalysts. *Catal. Today* **2013**, *215*, 60–66. [CrossRef]
11. Gavrilović, L.; Brandin, J.; Holmen, A.; Venvik, H.J.; Myrstad, R.; Blekkan, E.A. Deactivation of Co-Based Fischer–Tropsch Catalyst by Aerosol Deposition of Potassium Salts. *Ind. Eng. Chem. Res.* **2018**, *57*, 1935–1942. [CrossRef]
12. Gavrilović, L.; Brandin, J.; Holmen, A.; Venvik, H.J.; Myrstad, R.; Blekkan, E.A. Fischer-Tropsch synthesis—Investigation of the deactivation of a Co catalyst by exposure to aerosol particles of potassium salt. *Appl. Catal. B Environ.* **2018**, *230*, 203–209. [CrossRef]
13. Patanou, E.; Lillebø, A.H.; Yang, J.; Chen, D.; Holmen, A.; Blekkan, E.A. Microcalorimetric studies on Co-Re/γ-Al_2O_3 catalysts with na impurities for fischer-tropsch synthesis. *Ind. Eng. Chem. Res.* **2014**, *53*, 1787–1793. [CrossRef]
14. Olsen, B.K.; Kügler, F.; Castellino, F.; Jensen, A.D. Poisoning of vanadia based SCR catalysts by potassium: Influence of catalyst composition and potassium mobility. *Catal. Sci. Technol.* **2016**, *6*, 2249–2260. [CrossRef]
15. Chen, Q.; Svenum, I.-H.; Qi, Y.; Gavrilovic, L.; Chen, D.; Holmen, A.; Blekkan, E.A. Potassium adsorption behavior on hcp cobalt as model systems for the Fischer–Tropsch synthesis: A density functional theory study. *Phys. Chem. Chem. Phys.* **2017**, *19*, 12246–12254. [CrossRef]
16. Yang, J.; Frøseth, V.; Chen, D.; Holmen, A.; Frøseth, V.; Chen, D.; Holmen, A. Particle size effect for cobalt Fischer-Tropsch catalysts based on in situ CO chemisorption. *Surf. Sci.* **2016**, *648*, 67–73. [CrossRef]
17. Borg, Ø.; Dietzel, P.D.C.; Spjelkavik, A.I.; Tveten, E.Z.; Walmsley, J.C.; Diplas, S.; Eri, S.; Holmen, A.; Rytter, E. Fischer-Tropsch synthesis: Cobalt particle size and support effects on intrinsic activity and product distribution. *J. Catal.* **2008**, *259*, 161–164. [CrossRef]

18. Bezemer, G.L.; Bitter, J.H.; Kuipers, H.P.C.E.; Oosterbeek, H.; Holewijn, J.E.; Xu, X.; Kapteijn, F.; Van Diilen, A.J.; De Jong, K.P. Cobalt particle size effects in the Fischer-Tropsch reaction studied with carbon nanofiber supported catalysts. *J. Am. Chem. Soc.* **2006**, *128*, 3956–3964. [CrossRef]
19. Pendyala, V.R.R.; Jacobs, G.; Ma, W.; Klettlinger, J.L.S.; Yen, C.H.; Davis, B.H. Fischer-Tropsch synthesis: Effect of catalyst particle (sieve) size range on activity, selectivity, and aging of a Pt promoted Co/Al_2O_3 catalyst. *Chem. Eng. J.* **2014**, *249*, 279–284. [CrossRef]
20. Nakhaei Pour, A.; Housaindokht, M. Fischer-Tropsch synthesis over CNT supported cobalt catalysts: Role of metal nanoparticle size on catalyst activity and products selectivity. *Catal. Lett.* **2013**, *143*, 1328–1338. [CrossRef]
21. Arslan, I.; Walmsley, J.C.; Rytter, E.; Bergene, E.; Midgley, P.A. Toward three-dimensional nanoengineering of heterogeneous catalysts. *J. Am. Chem. Soc.* **2008**, *130*, 5716–5719. [CrossRef]
22. Rønning, M.; Tsakoumis, N.E.; Voronov, A.; Johnsen, R.E.; Norby, P.; Van Beek, W.; Borg, Ø.; Rytter, E.; Holmen, A. Combined XRD and XANES studies of a Re-promoted $Co/\gamma\text{-}Al_2O_3$ catalyst at Fischer-Tropsch synthesis conditions. *Catal. Today* **2010**, *155*, 289–295. [CrossRef]
23. Bao, A.; Li, J.; Zhang, Y. Effect of barium on reducibility and activity for cobalt-based Fischer-Tropsch synthesis catalysts. *J. Nat. Gas Chem.* **2010**, *19*, 622–627. [CrossRef]
24. Jacobs, G.; Das, T.K.; Zhang, Y.; Li, J.; Racoillet, G.; Davis, B.H. Fischer-Tropsch synthesis: Support, loading, and promoter effects on the reducibility of cobalt catalysts. *Appl. Catal. A. Gen.* **2002**, *233*, 263–281. [CrossRef]
25. Khodakov, A.Y.; Griboval-Constant, A.; Bechara, R.; Zholobenko, V.L. Pore size effects in Fischer Tropsch synthesis over cobalt-supported mesoporous silicas. *J. Catal.* **2002**, *206*, 230–241. [CrossRef]
26. Borg, Ø.; Eri, S.; Blekkan, E.A.; Storsæter, S.; Wigum, H.; Rytter, E.; Holmen, A. Fischer-Tropsch synthesis over γ-alumina-supported cobalt catalysts: Effect of support variables. *J. Catal.* **2007**, *248*, 89–100. [CrossRef]
27. Iglesia, E.; Soled, S.L.; Fiato, R.A. Fischer-Tropsch synthesis on cobalt and ruthenium. Metal dispersion and support effects on reaction rate and selectivity. *J. Catal.* **1992**, *137*, 212–224. [CrossRef]
28. Storsæter, S.; Borg, Ø.; Blekkan, E.A.; Holmen, A. Study of the effect of water on Fischer-Tropsch synthesis over supported cobalt catalysts. *J. Catal.* **2005**, *231*, 405–419. [CrossRef]
29. Wang, Z.-J.; Skiles, S.; Yang, F.; Yan, Z.; Goodman, D.W. Particle size effects in Fischer–Tropsch synthesis by cobalt. *Catal. Today* **2012**, *181*, 75–81. [CrossRef]
30. Azzam, K.; Jacobs, G.; Ma, W.; Davis, B.H. Effect of cobalt particle size on the catalyst intrinsic activity for fischer-tropsch synthesis. *Catal. Lett.* **2014**, *144*, 389–394. [CrossRef]
31. Den Breejen, J.P.; Radstake, P.B.; Bezemer, G.L.; Bitter, J.H.; Frøseth, V.; Holmen, A.; De Jong, K.P. On the Origin of the Cobalt Particle Size Effects in Fischer-Tropsch. *J. Am. Chem. Soc.* **2009**, *131*, 7197–7203. [CrossRef]
32. Brunauer, S.; Emmett, P.H.; Teller, E. Adsorption of Gases in Multimolecular Layers. *J. Am. Chem. Soc.* **1938**, *60*, 309–319. [CrossRef]
33. Barrett, E.P.; Joyner, L.G.; Halenda, P.P. The Determination of Pore Volume and Area Distributions in Porous Substances. I. Computations from Nitrogen Isotherms. *J. Am. Chem. Soc.* **1951**, *73*, 373–380. [CrossRef]
34. Jones, R.D.; Bartholomew, C.H. Improved flow technique for measurement of hydrogen chemisorption on metal catalysts. *Appl. Catal.* **1988**, *39*, 77–88. [CrossRef]
35. Patterson, A.L. The Scherrer formula for X-ray particle size determination. *Phys. Rev.* **1939**, *56*, 978–982. [CrossRef]
36. Schanke, D.; Vada, S.; Blekkan, E.A.; Hilmen, A.M.; Hoff, A.; Holmen, A. Study of Pt-Promoted Cobalt CO Hydrogenation Catalysts. *J. Catal.* **1995**, *156*, 85–95. [CrossRef]